Proceedings of the XVIII ECSMGE 2024
GEOTECHNICAL ENGINEERING CHALLENGES
TO MEET CURRENT AND EMERGING NEEDS OF SOCIETY

ISBN 978-1-032-54816-6
DOI 10.1201/9781003431749-90

Effects of physical characteristics on the shear behaviour of Foulum glaciofluvial sand

Effets des caractéristiques physiques sur le comportement en cisaillement du sable fluvio-glaciaire du Foulum

J.Z. Krabbe*
Aarhus University/NIRAS, Aarhus, Denmark

K.K. Sørensen
Aarhus University, Aarhus, Denmark

M.R. Lodahl
COWI, Aalborg, Denmark

**jzkr@niras.dk*

ABSTRACT: The geotechnical properties of sand deposits are heavily influenced by their physical characteristics, making their characterization essential. By subjecting 15 specimens to isotropic triaxial tests and by using a simple table scanner to collect 2D-oriented projections of the sand grains, the study aims to present a comprehensive physical characterization of Foulum high quartz glaciofluvial sand, with an emphasis on its implications on the shear behaviour and drained peak friction angle φ'_p of the tested sand. The results revealed the multifaceted nature of granular material behaviour. In particular, the stress dependency and initial conditions emerged as extremely important, in line with previous research. The study also highlights the importance of the sample size when considering particle shape (sphericity in particular) on the geotechnical properties.

RÉSUMÉ: Les propriétés géotechniques des sediments sableux sont fortement influencées par leurs caractéristiques physiques, ce qui rend leur caractérisation essentielle. En soumettant 15 spécimens à des essais triaxiaux isotropes et en utilisant un scanner à plat pour collecter des projections orientées en 2D des grains de sable, cette étude vise à présenter une caractérisation physique complète des sédiments fluvio-glaciaire à haute teneur en quartz de Foulum, en mettant l'accent sur ses implications sur le comportement au cisaillement et l'angle de frottement maximal drainé φ'_p des échantillons testés. Les résultats ont révélé les comportements très diversifiés des matériaux granulaires. En particulier, la dépendance aux contraintes et conditions initiales ont émergé comme étant extrêmement importantes, conformément aux études précédentes. L'étude met également en évidence l'importance de la taille de l'échantillon lors de la prise en compte de la forme des particules (en particulier la sphéricité) sur les propriétés géotechniques.

Keywords: Shear behaviour; triaxial tests; particle shape; sphericity; drained peak friction angle.

1 INTRODUCTION

Knowledge of the peak drained friction angle of sands φ'_p is important for the construction and safety of most geotechnical designs such as foundations, excavations, tunnels, slopes, and many other important civil engineering works. In contrast to the critical state friction angle, φ'_{cs}, the peak friction angle φ'_p is not a fundamental soil property but depends on the sands' capacity to dilate. Thus, it changes with mineralogy, particle shape, particle irregularities and distribution of soil particles, the magnitude of the effective confining stress, the initial void ratio, the applied stress path, and much more. This has led to the peak friction angle in designs being largely dependent on the geotechnical engineers' experience. Nevertheless, extensive studies (i.e., Bolton 1986, among others) have sought to formulate mathematical expressions for triaxial compression loading based on the confining stress, relative density, and fitting parameters based on the mineralogy and particle shape.

This study aims to characterise and link the physical and mechanical shearing properties of a Danish high quartz glaciofluvial sand. Additionally, the study seeks to investigate the extent to which experimental studies conducted on sands accurately reflect the geological context and variability, and how this can be better incorporated into subsequent analyses, with an emphasis on its implications on the shear behaviour and drained peak friction angle φ'_p.

2 TEST MATERIAL AND METHODS

The investigated “Foulum sand” is a natural high quartz glaciofluvial sand collected at the Foulum test site near the Danish glacial front line in the middle of Jutland, Denmark, from a depth of 2 m to 14 m.

The grain size distribution obtained using dry sieving method classifies the sand as a clean sand (FC < 5%) and poorly graded (SP) group according to the United Soil Classification System with a coefficient of uniformity $U = 2 - 4$ and a coefficient of curvature $Z <$ 1.3. Visual and chemical composition analysis showed that the mineral composition of Foulum Sand is dominated by Quartz (> 80%) in addition to feldspar. The specific gravity (G_s) was found to range between 2.62 to 2.67 (mean 2.64), accurately representing a mineral composition of primarily quartz and feldspar with some fines content present. Standard Danish laboratory procedures were used to determine the void ratio limits. The minimum void ratio e_{min} ranged from 0.36 to 0.52 (mean 0.44) the maximum void ratio e_{max} ranged from 0.72 to 1.01 (mean 0.8).

2.1 Experimental program and procedures

In addition to the standard index properties a detailed analysis has been carried out to characterise the particle shapes. Three main scales which define particle shape irregularities exist (considering a 2D projection). While sphericity is related to the ‘form’ and thus sensitive to particle elongation, roundness reflects the variations and sharpness of particle corners (i.e., angularity) and roughness describes surface texture at the smallest scale, cf. Figure 1a.

In this study a ‘CanoScan LiDE 300’ table scanner with a 1200 DPI resolution was used to facilitate the collection of 2D-oriented projections of sand grains. A sample size of least 1000 particles have been considered to capture the grain variability as suggested by Rorato (2019). After the scan was performed the image was prepared (increasing the image size) using the commercial program ImageJ Fiji (Schindelin et al. 2012) and subsequently binarised, segmented, and labelled using the open-source python package SPAM (Stamati et al. 2020) as shown in Figure 1b. The Python script originally developed by Rorato (2019) was used to compute the mean value and standard deviation of the distribution of 2D perimeter sphericity, S_p, of the grains.

In addition, the freely available commercial program ImageJ Fiji and the Particle8_Plus plugin (Landini 2008) have been used as an alternative method to determine the sphericity (S) and roundness (R) from square pixels to extract the features:

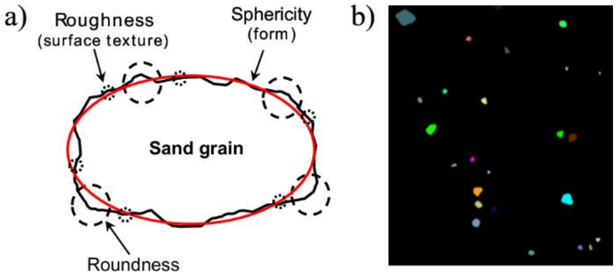

Figure 1. a) Particle shape characterisation at different scales, b) Obtained 2D-oriented projections of sand grains - Labelled image.

$$S = \frac{R_i}{R_c}, R = \frac{4A_c}{\pi L_{major}^2} \tag{1}$$

In Eq. (1) R_i is the radius of the inscribed circle, R_c is the radius of the circumscribed circle at the center of mass, A_c is the cross-sectional area, and L_{major} is the length of the major axis.

For examining the shear strength, 15 isotropically consolidated drained triaxial compression tests (CID) with pore water pressure measurements were performed on clean Foulum sand. The CID tests were dry reconstituted by the undercompaction method by Ladd (1978) and prepared using an equal height to diameter ratio (h/d = 1) while employing lubricated ends. The normally consolidated specimens were consolidated to an isotropic compression mean effective stress p'_c between 35 and 255 kPa.

3 LABORATORY TEST RESULTS

The index relationships and strength results for the tested Foulum sand specimens are presented in Table 1.

The computed mean values of S_p were found to range from 0.83 to 0.95 with a standard deviation between 0.03 to 0.06, indicating that the sand is highly spherical. Conversely, using the methodology presented in Eq. (1) the sphericities were found to vary between 0.61 to 0.68. This underscores the significance of the selected computational framework. The range of void ratio before shearing e_s varied from as low as 0.49 to as high as 0.82 (mean 0.62), corresponding to a relative density range of 38.2% < D_R < 66.6% with a mean of D_R = 49.8%.

The mean stress at failure, p'_f, was observed to be between 65 kPa to 577 kPa, resulting in normalised peak shear stresses q/p'_f in the range of 1.37 to 1.74, overall, with a tendency to increase in value for greater values of confining p'_c. Distinct dilative behaviour was obtained on specimens recompacted to D_R values higher than about 40%, generally attaining peak angle of dilation (ψ_p) values greater than 7° at observed peak

Table 1. Summary of index and strength properties for the tested specimens.

Nr.	Grain size distribution				Particle shape			Shearing state and properties						
	FC (%)[a]	D_{50} (mm)	U^b $(-)$	Z^c $(-)$	S_p $(-)$	S $(-)$	R $(-)$	D_R (%)	e_s $(-)$	p'_c (kPa)	p'_f (kPa)	ψ_p (°)	φ'_p (°)	φ'_{cs} (°)
1	2.30	0.37	2.92	1.18	0.91	0.66	0.58	39.0	0.82	35	65	0.9	34.0	33.4
2	2.41	0.34	2.87	1.18	0.93	0.66	0.58	41.5	0.76	53	101	3.8	35.1	32.9
3	0.85	0.57	2.56	0.87	0.92	0.67	0.60	53.5	0.57	71	169	14.9	42.3	35.3
4	2.71	0.46	3.32	1.12	0.89	0.68	0.59	56.1	0.55	81	191	14.2	41.5	34.9
5	2.03	0.51	2.93	1.00	0.88	0.65	0.58	54.2	0.56	90	204	11.9	41.0	34.8
6	5.78	0.49	4.57	1.30	0.85	0.63	0.55	40.4	0.58	99	215	11.1	39.5	34.7
7	2.23	0.47	3.25	1.09	0.95	0.67	0.60	52.2	0.57	125	276	12.4	40.1	34.6
8	2.47	0.46	2.93	1.06	0.86	0.68	0.61	65.5	0.52	146	349	14.0	42.5	35.0
9	4.03	0.36	3.13	1.21	0.84	0.67	0.60	38.2	0.73	43	82	3.6	34.0	32.2
10	2.53	0.35	2.72	1.27	0.87	0.65	0.57	43.2	0.67	88	182	9.2	37.5	33.1
11	2.89	0.34	2.88	1.22	0.85	0.64	0.57	48.8	0.63	107	230	9.6	38.6	33.4
12	3.36	0.39	3.26	1.21	0.83	0.66	0.58	51.8	0.59	126	258	8.2	37.2	33.4
13	3.69	0.38	3.29	1.22	0.87	0.64	0.56	48.6	0.61	144	289	6.7	36.7	33.5
14	4.72	0.33	3.12	1.05	0.93	0.64	0.58	46.8	0.66	225	422	2.4	34.3	33.2
15	4.67	0.19	2.51	1.03	0.83	0.64	0.58	66.6	0.49	255	577	13.6	40.7	34.3

[a]Fines content < 0.075mm; [b]Coefficient of uniformity $\boldsymbol{U = D_{60}/D_{10}}$; [c]Coefficient of curvature $\boldsymbol{Z = D_{30}^2/(D_{60} \times D_{10})}$

strength. In four cases, the reconstituted specimens showed contractive behaviour and much lower shear strength. The drained peak friction angles φ'_p were observed to lie between 34° to 42.5°, commonly reached at about an axial strain of $\varepsilon_a = 6 - 8\%$. The critical state friction angles φ'_{cs} were observed to lie between 32.2° to 35.3°, although some tests were not run to sufficiently large strains for a complete critical state to be reached. The level of dilatancy during shearing is presented in Figure 2a and are seen to vary approximately linearly with ψ_p giving the relationship $\varphi'_p = \varphi'_c + 0.48\psi_{max}$.

4 CORRELATIONS BETWEEN DATA

A multivariable linear regression analysis has been performed to investigate the interdependencies between the physical attributes of Foulum glaciofluvial sand and its shear behaviour. The sensitivity analysis presented in Table 2 highlights and serves as a valuable reference for understanding the observed trends.

The three parameters exerting the most significant influence on the φ'_p are e_s, $\ln p'_c$ and D_R. This is evidenced by low p-values at 1.6%, 1.8% and 6.2%, respectively, indicating a strong significance in the model and strong linear relationship. This is consistent with the work of Bolton (1986) and others, who demonstrated that for a given granular material, the difference $\varphi'_p - \varphi'_{cs}$ generally varies approxi-mately linearly with the logarithm of vertical stress. Moreover, the slope of this linear variation changes systematically with the sample's relative density.

Interestingly, the analysis revealed that incorporating S_p (6.2%) plays a more crucial role than S (10.8%) likely due to its equivalency to the 3D true sphericity for the 2D particle (Rorato 2019). Similar p-values of those attained by S are obtained by other various sphericity descriptors, such as the area-, diameter-, and ks sphericity. This highlights the importance of considering different measures of sphericity in geotechnical analysis and underscores the complexity of granular material behaviour. The influence of roundness was found insignificant. Of the particle shape properties, the roundness indicates the lowest level of statistical significance at 27.6%.

The grain size distribution (GSD) further revealed the importance of several other parameters, albeit to a lesser extent. The Z and D_{50} emerged as the most significant properties.

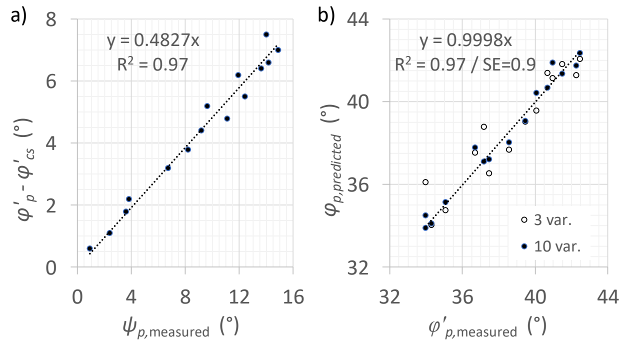

Figure 2. a) Level of dilatancy during shearing, b) measured vs. predicted peak drained friction angle φ'_p (trendline for 10 variables).

Table 2. Sensitivity analysis for φ'_p, φ'_{cs} and ψ_p. Percentages given for the properties indicate their respective p-values.

	Grain size distribution				**Particle shape**			**Shearing state and properties**			**Combined statistics**		
	FC (%)	D_{50} (%)	U (%)	Z (%)	S_p (%)	S (%)	R (%)	D_R (%)	e_s (%)	$\ln p'_c$ (%)	p (%)	SE (°)	R^2 (−)
φ'_p	21.4	13.2	16.2	8.9	6.2	10.8	27.6	6.2	1.6	1.8	1.00	0.92	0.97
φ'_{cs}	6.7	13.0	4.0	0.6	3.4	41.9	27.7	–	–	–	24.1	0.62	0.71
ψ_p	33.1	33.9	21.0	15.2	10.3	26.9	35.2	39.5	0.5	3.1	1.28	1.52	0.97

Figure 2b depicts the measured versus predicted peak drained friction angle φ'_p for 3 (shearing state properties) and 10 included variables. When considering the combined statistics of all the variables, the model was found to be statistically significant with a p-value of 0.95%. The R^2 value of 0.97 was found to provide a strong fit, ultimately resulting in a standard error (SE) of 0.92°. Thus, the variables included in the model appear to be good predictors, providing a robust and accurate model.

The variable φ'_{cs}, which is independent of shearing state and properties, reveals four index parameters (Z, S_p, U and FC) as particularly influential, with respective p-values of 0.6%, 3.4%, 4.0%, and 6.7%. This aligns with the critical state concept of dependence on factors such as mineralogy, particle shape and particle irregularities. It is noted that S_p emerges as vastly superior to S, while R also provides a low level of statistical significance. It is likely that the table scanner is not able to present a high enough quality scan for the algorithm to sufficiently capture the roundness. The combined variables yield a p-value of 24.1%, R^2 value of 0.71 and SE of 0.62°. These results are likely influenced by the fact that some tests were not performed at strains large enough to achieve a fully developed critical state.

In the sensitivity analysis conducted for the peak angle of dilation ψ_p, the variables exhibited varying degrees of statistical significance. As sands ability to exhibit dilating behaviour is directly related to shearing state and the applied confining pressure, it is unsurprisingly that e_s and $\ln p_c$ indicates a very strong significance with p-values of 0.5% and 3.1%, respectively. It is noteworthy that the inclusion of the last 8 variables only marginally increases the predictive abilities from an R^2 value of 0.92 to 0.97. This suggests that these variables, while contributing to the model, do not drastically improve its predictive power.

5 CONCLUSION

This study delves into the characterization of high quartz glaciofluvial sand through a meticulous examination of its physical and mechanical properties. The findings provide insights into the role of particle shape, in particular different measures of sphericity. Furthermore, the findings underscore the multifaceted nature of granular material behaviour and highlight the need for a comprehensive approach in geotechnical analysis that considers a wide range of parameters.

ACKNOWLEDGEMENTS

The authors would like to acknowledge the support from COWI fonden. Further, thank you to Marcos Arroyo from Universitat Politècnica de Catalunya (UPC), Riccardo Rorato (formerly at UPC) and Marco Previtali from the University of Dundee for providing the necessary scripts for image analysis.

REFERENCES

Bolton, M. D. (1986), The strength and dilatancy of sands, *Géotechnique,* 36(1), pp. 65-70, https://doi.org/10.1680/geot.1986.36.1.65.

Ladd, R. S. (1978), Preparing test specimens using undercompaction, *Geotechnical testing journal,* 1(1), pp. 16-23, https://doi.org/10.1520/GTJ10364J.

Landini, G. (2008), Advanced shape analysis with ImageJ, *Proceedings of the Second ImageJ user and developer Conference*, Available at https://blog.bham.ac.uk/intellimic/g-landini-software/, accessed: 08/10/2023.

Rorato, R. (2019), *Imaging and discrete modelling of sand shape,* Doctoral dissertation, Universitat Politècnica de Catalunya. Available at: https://upcommons.upc.edu, accessed: 08/10/2023.

Schindelin, J., Arganda-Carreras, I., Frise, E., Kaynig, V., Longair, M., Pietzsch, T., Preibisch, S., Rueden, C., Saalfeld, S., Schmid, B. and Tinevez, J.Y. (2012), Fiji: an open-source platform for biological-image analysis, *Nature methods*, 9(7), pp. 676-682. https://doi.org/10.1038/nmeth.2019.

Stamati, O., Andò, E., Roubin, E., Cailletaud, R., Wiebicke, M., Pinzon, G., Couture, C., Hurley, R.C., Caulk, R., Caillerie, D. and Matsushima, T. (2020), Spam: software for practical analysis of materials, *Journal of Open Source Software*, 5(51), 2286, https://doi.org/10.21105/joss.02286.